Int. J. Electron. Commun. (AEÜ) 107 (2019) 199–208

Contents lists available at ScienceDirect

International Journal of Electronics and Communications (AEÜ)

journal homepage: www.elsevier.com/locate/aeue

Regular paper

Performance analysis of repeated index modulation for OFDM with MRC and SC diversity under imperfect CSI

Thi Thanh Huyen Le, Xuan Nam Tran *

Faculty of Radio Electronics, Le Quy Don Technical University, Hanoi, Viet Nam

ARTICLE INFO

Article history:
Received 27 December 2018
Accepted 15 May 2019

Keywords:
Index modulation for OFDM
Spatial diversity
Frequency diversity
Maximum likelihood detection
Symbol error probability
Imperfect CSI

ABSTRACT

In this paper, we conduct the investigation into the performance of repeated index modulation-orthogonal frequency division multiplexing (RIM-OFDM) system with spatial diversity comprising the maximal ratio combining (MRC) and selection combining (SC). The considered systems, abbreviated as RIM-OFDM-MRC and RIM-OFDM-SC, are successful in exploiting both the frequency and spatial diversities to provide improvement in the error performance of the conventional IM-OFDM system with diversity reception. We find out the closed-form expressions for the index and symbol error probabilities of RIM-OFDM-MRC and RIM-OFDM-SC under a variety of different channel conditions. We also carry out asymptotic analysis in order to examine the system behavior under influences of system parameters and the imperfection in channel state information (CSI). Performance evaluation through both theoretical and simulation results demonstrates the significant performance improvement of our systems in comparison with the conventional IM-OFDM using MRC/SC even when channel estimation errors occur at the receiver.

1. Introduction

Orthogonal frequency division multiplexing (OFDM) is a well-known multi-carrier modulation technique, which can eliminate interference between symbols and provide high spectral efficiency. Recently, researchers have shown an increased interest in introducing novel OFDM schemes to improve the performance of the original OFDM. Several latest works may be mentioned as adaptive modulation for space frequency block code-OFDM [1], spatial modulation-OFDM [2], space time block code-OFDM [3]. Additionally, index modulation for OFDM (IM-OFDM) has emerged as an advanced OFDM technique which can improve the error performance, energy and spectral efficiency of the traditional OFDM [4]. In comparison with OFDM, IM-OFDM only activates a number of sub-carriers and utilizes both the *M*-ary modulated symbols and indices of active sub-carriers to convey data bits.

Since the original IM-OFDM system was reported in [5], the issue of IM-OFDM has received considerable critical attention. In [4], the trade-off between the spectral efficiency and error performance was insured by utilizing flexible adjustment of active sub-carriers. Taking care of the reliability, the authors in [6] employed sub-carrier interleaving to expand the Euclidean distance between the *M*-ary modulated symbols, thus decreased its bit error probability.

In another approach, Fan et al. introduced the simultaneous in-phase and quadrature index modulation for OFDM (IQ-IM-OFDM) that could improve the spectral efficiency [7]. The work in [8] was successful in exploiting inactive sub-carriers to transmit extra information bits. Extending this idea, the multi-mode IM-OFDM was reported in [9]. This proposal can further improve the spectral efficiency by activating all sub-carriers and utilizing a variety of distinct modes and their permutations to carry data bits.

In order to simplify the system structure, a greedy detector for IM-OFDM was found. Beside that, its bit error rate (BER) was analyzed in the presence of uncertain channel state information (CSI) [10]. Researchers in [11] attempted to evaluate the impact of channel estimation errors on the symbol error probability (SEP) of IM-OFDM using both the maximum likelihood (ML) and greedy detectors. Moreover, the performance investigation of IM-OFDM schemes has been attracting a lot of interest. Particularly, the average bit error probability of IM-OFDM was evaluated in [4]. The mathematical expressions for BER of IM-OFDM were successfully derived in [12]. The paper [13] examined the outage probability of IM-OFDM over two-way diffused-power fading channels.

* Corresponding author at: Le Quy Don Technical University, 236 Hoang Quoc Viet, Bac Tu Liem, Hanoi, Viet Nam.
E-mail addresses: huyen.ltt@mta.edu.vn (T.T.H. Le), namtx@mta.edu.vn (X.N. Tran).

https://doi.org/10.1016/j.aeue.2019.05.022
1434-8411/

Regarding the diversity issue, the transmit diversity can be obtained by delivering the real and imaginary parts of complex data symbols over two separated active sub-carriers [14]. Using a different approach, the linear constellation pre-coding for IM-OFDM was reported in [15] to enhance not only the diversity gain but also the spectral efficiency. The study in [16] dealt with diversity reception for IM-OFDM combining with greedy detection for device to device communications sytems to increase the diversity gain at low complexity. The repetition of index symbol for IM-OFDM to achieve transmit diversity can be found in [17].

In order to further improve the spatial diversity gain and the reliability, a number of authors have considered the combination between IM-OFDM and multiple input multiple output (MIMO) systems. The MIMO-IM-OFDM scheme was found in [18]. Moreover, in [18], maximum likelihood (ML), near-ML, minimum mean square error (MMSE) and ordered successive interference cancellation (OSIC) detectors for MIMO-IM-OFDM was also proposed. In order to exploit the diveristy of MIMO-OFDM-IM, a recent scheme which combines MIMO-OFDM-IM with space-frequency code was introduced in [19]. Detectors based on the sequential Monte Carlo (SMC) were designed for MIMO-OFDM-IM which can achieve the near-optimal error performance at low complexity in [20]. In order to deal with multi-antenna and multi-user interference, the study in [22] proposed the use of the turbo receiver for MIMO-IM-OFDM system which not only efficient in equalizing, decoding, but also in channel estimation.

Although extensive researches have been carried out on IM-OFDM, no single study exploits simultaneously both frequency and spatial diversities. Whilst various studies confirmed the effectiveness of exploitation of spatial diversity, very little attention has been paid to frequency diversity.

Motivated by this fact, we extend two enhanced IM-OFDM schemes using maximal ratio combining (MRC) and selection combining (SC), which are successful in simultaneous exploiting the spatial and frequency diversities to further improve the diversity gain and the transmission reliability of IM-OFDM with diversity reception for D2D communications. Nevertheless, in the previous work [21], we have not provided an analysis in much detail for SEP performance of our proposed schemes. There has been no detailed investigation of the impacts of system configure on the reliability. Beside that, this study focuses on dealing only with channel whose state information was estimated perfectly in the receiver. For more practical scenarios, imperfect channel state information (CSI) has much effect on the SEP performance of the system. In the literature, various researches have focused on channel estimation for the OFDM system. Channel estimation based on pilot symbols can be found [23,24]. However, not all sub-carriers are activated in the IM-OFDM system, thus, the techniques applied to the OFDM system will be different from OFDM-IM due to sub-carrier activation that depends on the index bits. The authors in [25] proposed a novel method with interpolation for IM-OFDM to estimated the channel responds at activated sub-carriers. In order to estimate the channel according to the data symbols, a number of interpolation techniques, such as nearest interpolation, piecewise linear interpolation, piecewise cubic Hermite, FFT interpolation and low-pass interpolation can be utilized. In another work, the Kalman channel estimation for the MIMO-IM-OFDM system was proposed in [22] which attains not only efficiency but also low complexity.

Under scenario of a point-to-point communication system aided by IM-OFDM which requires the not only high reliability but also low complexity and considering all of these evidences, this paper discovers the novel IM-OFDM schemes which can considerably increase the transmission reliability, even in the presence of imperfect CSI and critically examine the dependences of the system on the various different configurations. The main contributions of our work are summarized as follows.

- We propose new IM-OFDM schemes combining repeated transmission with MRC/SC receive diversities (referred to as RIM-OFDM-MRC and RIM-OFDM-SC), which can attain simultaneously spatial and frequency diversity gain.
- For the purpose of analysis, the closed-form expressions for the symbol error probability (SEP) of index symbols and M-ary modulated symbols and average SEP for RIM-OFDM-MRC/SC under imperfect CSI condition are successfully derived.
- Asymptotic analysis for the SEP of the proposed schemes is also conducted to investigate the effects of system parameters, comprising the number of active sub-carriers, receive antennas, modulation size and channel estimation errors on the SEP. The analytical results recommend us to select an optimum scheme with the best performance thanks to appropriate parameters.
- The error performance of RIM-OFDM-MRC/SC are evaluated via both simulation and analytical results. The evaluation results prove the superior error performance of our proposed schemes over the conventional IM-OFDM-MRC and IM-OFDM-SC at the same spectral efficiency.

The remainder of this paper proceeds as follows. Section 2 describes the system model of the considered RIM-OFDM-MRC/SC. The closed-form expressions of IEP and SEP in the cases of perfect and imperfect CSI are derived in Sections 3 and 4, respectively. Performance evaluation is given in Section 5. Finally, Section 6 concludes the paper.

Notation: Upper and lower case boldface letter stands for matrices and column vectors, respectively, $C(N,K)$ is the K combination of N. $(.)^T$ and $\lfloor . \rfloor$ denote the transpose and floor operations, respectively. $\mathbb{E}(z), \mathcal{M}_z(.)$ refer to the expectation operation and the moment generating function of random variable x, respectively.

2. System model

We address an up-link SIMO-IM-OFDM system as given in Fig. 1. The transmitter is equipped with a single antenna while the receiver has L antennas for diversity reception. The system uses a total of N_F sub-carriers which are separated into G sub-blocks of N sub-carriers, i.e., $N = N_F/G$. In comparison with the IM-OFDM system, each sub-block also activates only K out of N sub-carriers and leaves the remaining sub-carriers for zero padding. However, all active sub-carriers in our proposed scheme transmit the same M-ary modulated symbol s. This repeated modulation over the sub-carrier domain is used to obtain frequency diversity at the expense of the spectral efficiency. At the receiver, MRC or SC can be used for reception combining in order to attain spatial diversity.

For high-rate OFDM systems, the sub-carrier spacing becomes large, making sub-blocks operate independently. Without loss of generality, let us consider the operation of one sub-block. During the transmission of each sub-block, input bits to the transmitter are divided into two parts.

The first part, which comprises $p_1 = \lfloor \log_2 C(N,K) \rfloor$ bits, are fed to the index modulator to determine K active sub-carrier indices. Let θ denote the set of indices of active sub-carriers, $\theta = \{\alpha_1, \ldots, \alpha_K\}$, where $\alpha_k \in \{1, \ldots, N\}$ represents the index of the k-th sub-carrier, $k = 1, \ldots, K$. For the given N and K, there are a total of $c = 2^{\lfloor \log_2 C(N,K) \rfloor}$ active index combinations. Using θ we can define an index symbol by a vector $\boldsymbol{\lambda} = [\beta_1, \ldots, \beta_N]^T$, where $\beta_i = 1$ for $i \in \theta$, and $\beta_i = 0$ for $i \notin \theta$. These index symbols can be generated by the combination method [4].

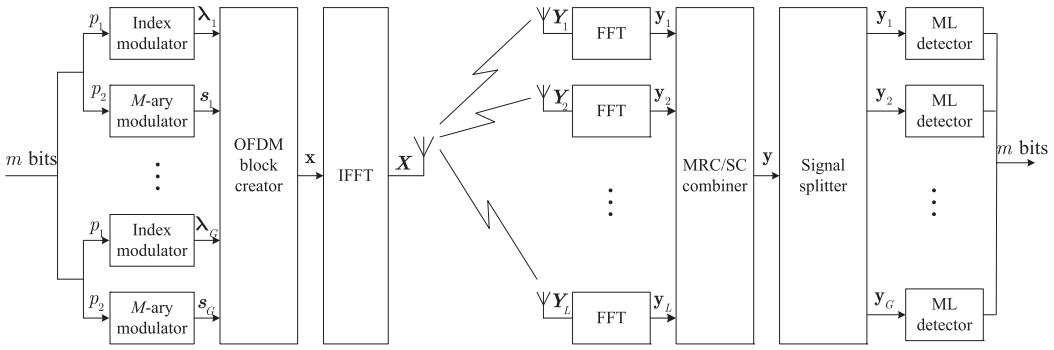

Fig. 1. Structure of the RIM-OFDM-MRC/SC transceiver.

The remaining part of input bits, which consists of $p_2 = \log_2 M$ bits, are used for the M-ary modulation to obtain symbol s. Based on the index symbol and the data symbol, the transmitted signal vector $\mathbf{x}$ is generated as $\mathbf{x} = \boldsymbol{\lambda} s$. Consequently, the number of transmitted bits in each sub-block are equal to $p = p_1 + p_2$ bits, which results in the spectral efficiency attained by

$$\bar{\varrho} = \frac{1}{N}(\lfloor \log_2 C(K,N) \rfloor + \log_2 M)[\text{bps/Hz}]. \tag{1}$$

At the receiver, the received signal over N sub-carriers at the l-th antenna is given by

$$\mathbf{y}_l = \mathbf{H}_l \mathbf{x} + \mathbf{n}_l = \mathbf{H}_l \boldsymbol{\lambda} s + \mathbf{n}_l, \tag{2}$$

where $\mathbf{y}_l = [y_l(1), \ldots, y_l(N)]^T$, $l = 1, \ldots, L$; $\mathbf{H}_l = \text{diag}(h_l(1), \ldots, h_l(N))$ is the channel matrix between the transmitter and the l-th receive antenna. Each element $h_l(\alpha)$, where $\alpha = 1, 2, \ldots, N$, is an independent complex-valued Gaussian random variable with $h_l(\alpha) \sim \mathcal{CN}(0,1)$. The additive Gaussian noise vector $\mathbf{n}_l = [n(1), \ldots, n(N)]^T$ has its elements $n_l(\alpha) \sim \mathcal{CN}(0, N_0)$, where N_0 is the noise variance. It is assumed that $\mathbb{E}\left\{|s|^2\right\} = \varphi E_s$, where E_s describes the average energy per the M-ary modulated symbol; $\varphi = N/K$ is the power allocation coefficient. Under this assumption, the average signal-to-noise ratio (SNR) per active sub-carrier can be defined as $\bar{\gamma} = \varphi E_s / N_0$.

After the fast Fourier transform (FFT), either MRC or SC is used to combine the received signals from L antennas as illustrated in Fig. 1. The output of the reception combiner can be expressed as

$$\mathbf{y} = \mathbf{H} \boldsymbol{\lambda} s + \mathbf{n}, \tag{3}$$

where $\mathbf{y} = \{\mathbf{y}_{\text{MRC}}, \mathbf{y}_{\text{SC}}\}, \mathbf{H} = \{\mathbf{H}_{\text{MRC}}, \mathbf{H}_{\text{SC}}\}, \mathbf{n} = \{\mathbf{n}_{\text{MRC}}, \mathbf{n}_{\text{SC}}\}$ which depends on the receiver side employs MRC or SC. Specifically, the combiner output in the MRC and SC scenario is described as follows.

2.0.1. RIM-OFDM-MRC

Using a weighted matrix $\mathbf{W} = \mathbf{H}^H$, the output of the MRC is given by

$$\mathbf{y}_{\text{MRC}} = \mathbf{H}_{\text{MRC}} \boldsymbol{\lambda} s + \mathbf{n}_{\text{MRC}}, \tag{4}$$

where $\mathbf{H}_{\text{MRC}} = \mathbf{WH}$ is the equivalent channel matrix, $\mathbf{H} = \left[\mathbf{H}_1^T, \ldots, \mathbf{H}_L^T\right]^T$; $\mathbf{n}_{\text{MRC}} = \mathbf{Wn}$ is the noise vector at the output of the MRC combiner, $\mathbf{n} = \left[\mathbf{n}_1^T, \ldots, \mathbf{n}_L^T\right]^T$ represents the noise vector per diversity branch.

2.0.2. RIM-OFDM-SC

The SC combiner chooses one of the diversity branches which has the largest SNR. The output of the SC combiner is given by $\mathbf{y}_{\text{SC}} = \mathbf{H}_{\text{SC}} \boldsymbol{\lambda} s + \mathbf{n}_{\text{SC}}$, where $\mathbf{H}_{\text{SC}} = \text{diag}(h_{\text{SC}}(1), \ldots, h_{\text{SC}}(N))$ with each element $h_{\text{SC}}(k) = \max_l |h_l(k)|^2$, for $k = 1, \ldots, N$ and $\mathbf{n}_{\text{SC}}$ denotes the noise vector at the largest SNR.

The received signal vector $\mathbf{y}$ is then split into G the sub-vectors $\mathbf{y}_g$, $g = 1, \ldots, G$, corresponding to the designated sub-blocks. The sub-block signals are expressed as $\mathbf{y}_g = \mathbf{H}_g \boldsymbol{\lambda} s + \mathbf{n}_g$, where $\mathbf{H}_g$ and $\mathbf{n}_g$ are the channel matrix and the noise vector at the sub-block g, respectively. The ML detection are then applied to these signals to estimate both the indices of the active sub-carriers and the M-ary modulated symbol.

For signal recovery, a ML detector is employed to jointly estimate the index symbols and the M-ary modulated symbol s from all transmitted RIM-OFDM-MRC/SC signals. The estimated index symbol vector and the M-ary modulated symbol vector are given by

$$\left(\hat{\boldsymbol{\lambda}}, \hat{s}\right) = \arg\min_{\boldsymbol{\lambda}, s} \|\mathbf{y} - \mathbf{H} \boldsymbol{\lambda} s\|^2. \tag{5}$$

3. Performance analysis Of RIM-OFDM-MRC/SC under perfect CSI

In this section, we analyze the symbol error probability of the two proposed schemes, i.e., RIM-OFDM-MRC and RIM-OFDM-SC using the ML detection under the assumption of without channel estimation error at the receiver. The term "symbol error probability (SEP)" has been used to describe the ratio of the number of erroneous symbols to a total of number of transmitted symbols. The SEP, denoted by P_s, is separated into two parts: index symbol error probability P_I and the M-ary modulated symbol error probability P_M. The respective average probabilities are denoted by $\overline{P}_s, \overline{P}_I$ and $\overline{P}_M$.

3.1. Performance analysis for RIM-OFDM-MRC

3.1.1. Index error probability

Firstly, we address the index error probability (IEP) by applying the pairwise index error probability (PIEP) of the ML detector. By definition, the PIEP is the probability that the detector makes a wrong estimation on a transmitted i-th index vector by the j-th index vector. It is supposed that the envelope of the M-ary PSK symbol is $|s| = \sqrt{\varphi E_s}$. The PIEP can be then expressed by

$$P(\boldsymbol{\lambda}_i \to \boldsymbol{\lambda}_j) = Q\left(\sqrt{\frac{\varphi E_s \|\mathbf{H}\boldsymbol{\lambda}_i - \mathbf{H}\boldsymbol{\lambda}_j\|^2}{2N_0}}\right), \tag{6}$$

where $\boldsymbol{\lambda}_i$ and $\boldsymbol{\lambda}_j$ respectively represent the transmitted and the estimated index vector.

$Q(x) = \frac{1}{\sqrt{2\pi}} \int_x^\infty \exp\left(-\frac{y^2}{2}\right) dy$ is tail distribution function of the standard normal distribution [26]. Based on distance of $2D$ between $\boldsymbol{\lambda}_i$ and $\boldsymbol{\lambda}_j$, Eq. (6) can be rewritten as

$$P(\boldsymbol{\lambda}_i \to \boldsymbol{\lambda}_j) = Q\left(\sqrt{\frac{\sum_{d=1}^{D} \gamma_{\alpha_d}^{\mathrm{MRC}} + \gamma_{\tilde{\alpha}_d}^{\mathrm{MRC}}}{2}}\right), \tag{7}$$

where $\alpha_d^{\mathrm{MRC}} \in \theta_i$, $\tilde{\alpha}_d^{\mathrm{MRC}} \in \theta_j$, $\alpha_d^{\mathrm{MRC}}, \tilde{\alpha}_d^{\mathrm{MRC}} \notin \theta_i \cap \theta_j$, α and $\tilde{\alpha}$ denote the active and inactive sub-carrier; θ_i and θ_j represent corresponding index sets $\boldsymbol{\lambda}_i$, $\boldsymbol{\lambda}_j$, respectively. The instantaneous SNR per sub-carrier α is described by $\gamma_\alpha = \bar{\gamma}|h(\alpha)|^2$. Then, by applying the union bound, we can attain the index error probability of $\boldsymbol{\lambda}_i$ as follows

$$P_{I_i}^{\mathrm{MRC}} \leqslant \sum_{j=1, j\neq i}^{c} P(\boldsymbol{\lambda}_i \to \boldsymbol{\lambda}_j). \tag{8}$$

Therefore, the instantaneous PIEP of RIM-OFDM-MRC can be represented by

$$P_I^{\mathrm{MRC}} = \frac{1}{c}\sum_{i=1}^{c} P_{I_i}^{\mathrm{MRC}} \leqslant \frac{1}{c}\sum_{i=1}^{c}\sum_{j=1, j\neq i}^{c} P(\boldsymbol{\lambda}_i \to \boldsymbol{\lambda}_j). \tag{9}$$

Denote the set of indices $j, (j \neq i)$ by Ω_i such that $\boldsymbol{\lambda}_j$ satisfies the Hamming distance of 2 with $\boldsymbol{\lambda}_i$, i.e., $D = 1$. Let η_i represent a set of sub-carriers that their corresponding indices belong to Ω_i. From Eqs. (7) and (8), with $P_{I_i}^{\mathrm{MRC}}$ is bound by the condition $P(\boldsymbol{\lambda}_i \to \boldsymbol{\lambda}_j | j \in \Omega_i)$, i.e.,

$$\sum_{j=1, j\neq i}^{c} P(\boldsymbol{\lambda}_i \to \boldsymbol{\lambda}_j) \approx \sum_{j\in\Omega_i} P(\boldsymbol{\lambda}_i \to \boldsymbol{\lambda}_j).$$

The approximated expression of the instantaneous PIEP in (9) can be given by

$$P_I^{\mathrm{MRC}} \leqslant \frac{1}{c}\sum_{i=1}^{c}\sum_{j\in\Omega_i} P(\boldsymbol{\lambda}_i \to \boldsymbol{\lambda}_j) = \frac{1}{c}\sum_{i=1}^{c}\sum_{j\in\Omega_i} P(\alpha \to \tilde{\alpha}), \tag{10}$$

where $P(\alpha \to \tilde{\alpha}) = Q\left(\sqrt{\frac{\gamma_\alpha^{\mathrm{MRC}} + \gamma_{\tilde{\alpha}}^{\mathrm{MRC}}}{2}}\right) = Q\left(\sqrt{\frac{\gamma_\Sigma^{\mathrm{MRC}}}{2}}\right)$ describes the PIEP of incorrectly estimating an active sub-carrier $\alpha^{\mathrm{MRC}} \in \theta_i$ by an inactive sub-carrier $\tilde{\alpha}^{\mathrm{MRC}} \in \theta_j$, $\gamma_\Sigma^{\mathrm{MRC}} = \gamma_\alpha^{\mathrm{MRC}} + \gamma_{\tilde{\alpha}}^{\mathrm{MRC}}$. Hence, the average PIEP of RIM-OFDM-MRC can be attained by

$$P_I^{\mathrm{MRC}} \leqslant \frac{1}{c}\sum_{i=1}^{c}\sum_{j\in\Omega_i} \mathbb{E}_{\gamma_\Sigma^{\mathrm{MRC}}}\left\{Q\left(\sqrt{\frac{\gamma_\Sigma^{\mathrm{MRC}}}{2}}\right)\right\}. \tag{11}$$

Utilizing the approximation of $Q(x) \approx \frac{1}{12}e^{-\frac{x^2}{2}} + \frac{1}{4}e^{-\frac{2}{3}x^2}$ [27], the average PIEP can be expressed by

$$\overline{P}_I^{\mathrm{MRC}} \approx \mathbb{E}_{\gamma_\Sigma^{\mathrm{MRC}}}\left\{\vartheta\left(\frac{1}{12}e^{-\frac{\gamma_\Sigma^{\mathrm{MRC}}}{4}} + \frac{1}{4}e^{-\frac{\gamma_\Sigma^{\mathrm{MRC}}}{3}}\right)\right\}, \tag{12}$$

where $\vartheta = \frac{\sum_{i=1}^{c}\eta_i}{c}$. Applying the definition and properties of the moment generating function (MGF): $\boldsymbol{\mathcal{M}}_\gamma(z) = \mathbb{E}_\gamma\{e^{-z\gamma}\}$ [26]. The MGF of $\gamma_\Sigma^{\mathrm{MRC}}$ can be determined by

$$\boldsymbol{\mathcal{M}}_{\gamma_\Sigma^{\mathrm{MRC}}}(z) = \boldsymbol{\mathcal{M}}_\gamma^{2L}(z) = (1 - z\bar{\gamma})^{-2L}. \tag{13}$$

Accordingly, we obtain the average PIEP of RIM-OFDM-MRC as follows

$$\begin{aligned}\overline{P}_I^{\mathrm{MRC}} &\approx \tfrac{\vartheta}{12}\left[\boldsymbol{\mathcal{M}}_{\gamma_\Sigma^{\mathrm{MRC}}}\left(-\tfrac{1}{4}\right) + 3\boldsymbol{\mathcal{M}}_{\gamma_\Sigma^{\mathrm{MRC}}}\left(-\tfrac{1}{3}\right)\right] \\ &= \tfrac{\vartheta}{12}\left[\tfrac{4^{2L}}{(4+\bar{\gamma})^{2L}} + \tfrac{3^{2L+1}}{(3+\bar{\gamma})^{2L}}\right].\end{aligned} \tag{14}$$

It is apparent from Eq. (14) that the average PIEP is only effected by N and K via $\bar{\gamma} = \frac{NE_s}{KN_0}$ and $c = 2^{\lfloor \log_2 C(N,K) \rfloor}$ without being influenced by the modulation order M. Furthermore, with given values of N and K, the PIEP is only affected by the index symbol $\boldsymbol{\lambda}$ via $\sum_{i=1}^{c}\eta_i$ and the number of receive antennas L.

3.1.2. M-ary modulated symbol error probability

The M-ary SEP is the probability that the receiver mis-estimates an M-ary modulated symbol while the indices of active sub-carriers are detected correctly. The instantaneous SEP of the M-ary modulated symbol is given by [26]

$$\overline{P}_M^{\mathrm{MRC}} \approx 2Q\left(\sqrt{2\gamma_{\Sigma,\alpha}^{\mathrm{MRC}}}\sin(\pi/M)\right), \tag{15}$$

where $\gamma_{\Sigma,\alpha}^{\mathrm{MRC}} = \sum_{l=1}^{L}\sum_{k=1}^{K}\gamma_{l,\alpha_k}$ and $\alpha_k \in \theta_i$. Then, applying the approximation of Q-function [27], $\overline{P}_M$ of the RIM-OFDM-MRC scheme can be represented by

$$\overline{P}_M^{\mathrm{MRC}} \approx \frac{1}{6}\left(e^{-\rho\gamma_{\Sigma,\alpha}^{\mathrm{MRC}}} + 3e^{-\frac{4\rho\gamma_{\Sigma,\alpha}^{\mathrm{MRC}}}{3}}\right), \tag{16}$$

where $\rho = \sin^2(\pi/M)$. Employing the MGF approach for the random variable $\gamma_{\Sigma,\alpha}^{\mathrm{MRC}}$, the MGF of $\gamma_{\Sigma,\alpha}^{\mathrm{MRC}}$ can be given by

$$\boldsymbol{\mathcal{M}}_{\gamma_{\Sigma,\alpha}^{\mathrm{MRC}}}(z) = \boldsymbol{\mathcal{M}}_\gamma^{LK}(z) = (1 - \bar{\gamma}z)^{-LK}. \tag{17}$$

Eq. (16) now can be rewritten as

$$\overline{P}_M^{\mathrm{MRC}} \approx \frac{1}{6}\left[\frac{1}{(1+\rho\bar{\gamma})^{LK}} + \frac{3}{\left(1+\frac{4\rho\bar{\gamma}}{3}\right)^{LK}}\right]. \tag{18}$$

In general, a symbol is erroneous when the index symbol and/or the M-ary modulated symbol are/is estimated inaccurately. Thus, the instantaneous SEP of RIM-OFDM-MRC and its average value are given by

$$P_s \approx \frac{1}{2c}\sum_{i=1}^{c}\left[P_M + \sum_{j\in\Omega_i} P(\alpha \to \tilde{\alpha})\right], \tag{19}$$

$$\overline{P}_s \approx \frac{\overline{P}_I + \overline{P}_M}{2}. \tag{20}$$

From Eq. (14), (18) and (19), the average SEP for the RIM-OFDM-MRC system can be approximated by

$$\begin{aligned}\overline{P_s}^{\mathrm{MRC}} \leqslant{}& \frac{\vartheta}{24}\left[\frac{16^L}{(4+\bar{\gamma})^{2L}} + \frac{3^{2L+1}}{(3+\bar{\gamma})^{2L}}\right] \\ &+ \frac{1}{12}\left[\frac{1}{(1+\rho\bar{\gamma})^{LK}} + \frac{3}{\left(1+\frac{4\rho\bar{\gamma}}{3}\right)^{LK}}\right].\end{aligned} \tag{21}$$

Eq. (21) indicates that for large $\bar{\gamma}$, $\bar{P}_s^{\mathrm{MRC}}$ is a function of $\bar{\gamma}^{-2L}$. This implies that the RIM-OFDM-MRC system can achieve diversity order of $2L$. This conclusion will be proved in the asymptotic analysis.

3.1.3. Asymptotic analysis

From (21), at high SNRs, the approximated expression for the SEP of RIM-OFDM-MRC in the case of the perfect CSI can be written as

$$\begin{aligned}\overline{P_s}^{\mathrm{MRC}} &\approx \left(\tfrac{K}{N}\right)^{2L}\tfrac{4^{2L}+3^{2L+1}}{24}\left(\vartheta + \tfrac{2\xi}{(4\rho)^{2L}}\right)\left(\tfrac{1}{\gamma_0}\right)^{2L}, \\ &= \Gamma\left((\gamma_0)^{-2L}\right)\end{aligned} \tag{22}$$

where $\gamma_0 = K\bar{\gamma}/N$ is the average SNR per sub-carrier, and $\xi = 1$ when $K = 2$, $\xi = 0$ for $K > 2$. Eq. (22) allows us to have an important insight into the dependence of the SEP on the system configuration as in remarks below.

Remark 1. For given values of N, K and γ_0, RIM-OFDM-MRC attains the diversity order of $2L$. The SEP is decreased when increasing L. For a large L, the average SEP exponentially comes down with the reduction of K/N. In order to improve the error performance, for a given L, we can choose the values of N and K such that K/N is small, i.e, select small N then small K and vice versa. Consequently, for a given γ_0, the best performance of RIM-OFDM-MRC can be achieved by jointly selecting a large L and smallest value of K/N.

Remark 2. For $K > 2$, we attain $\overline{P}_s^{\mathrm{MRC}} \approx \frac{\overline{P}_I^{\mathrm{MRC}}}{2}$. When $K = 2$, for a large L and given values of γ_0, N, K, a selection of large M will make the SEP exponentially increase through $\rho = \sin^2(\pi/M)$. Choosing a small $M(M = 2, 4)$ leads to $\overline{P}_s^{\mathrm{MRC}} \approx \frac{\overline{P}_I^{\mathrm{MRC}}}{2}$. Hence, $K > 2$ or $K = 2$ but M is small, the SEP at large SNR mostly depends on the index symbol estimation but not on estimation of the M-ary modulated symbol.

Remark 3. For given N, L and low spectral efficiency, i.e., small M, increasing K will make the reliability of RIM-OFDM-MRC reduced. The best performance can be attained by selecting $K = 2$. Nevertheless, this observation is no longer true when M is high ($M \geqslant 16$). In particular, the higher K will make the error performance better. Thus, these recommend that selecting K not higher than 2 when M is small and high K for large M will attain the best system configuration. In the RIM-OFDM-SC scheme, we also have the same statement which will be verified by the simulation in next section.

3.2. Performance analysis for RIM-OFDM-SC

3.2.1. Index error probability

For the RIM-OFDM-SC system, we apply the same calculation methodology as for RIM-OFDM-MRC. However, RIM-OFDM-SC only chooses the diversity branch which has the largest SNR. The instantaneous SNR of RIM-OFDM-SC can be found out by employing the probability density function (PDF) of the effective SNR for SC described in [16]

$$f_\gamma(\gamma_\alpha) = \frac{L}{\bar{\gamma}} \sum_{l=0}^{L-1} \binom{L-1}{l} (-1)^l e^{-\gamma_\alpha \frac{l+1}{\bar{\gamma}}}. \tag{23}$$

It is remarkable that $\gamma_\alpha^{\mathrm{SC}} = \max_{l=1,L} \gamma_{l,\alpha}^{\mathrm{SC}}$, where the instantaneous SNR of the l-th antenna at sub-carrier α is described by $\gamma_{l,\alpha}^{\mathrm{SC}}$. By conducting the inverse Laplace transform, the MGF of the random variable $\gamma_\alpha^{\mathrm{SC}}$ can be expressed by

$$\mathcal{M}_{\gamma_\alpha^{\mathrm{SC}}}(z) = L \sum_{l=0}^{L} \binom{L-1}{l} \frac{(-1)^l}{l+1-z\bar{\gamma}}. \tag{24}$$

The MGF of $\gamma_\Sigma^{\mathrm{SC}} = \gamma_\alpha^{\mathrm{SC}} + \gamma_\alpha^{\mathrm{SC}}$ can be given by $\mathcal{M}_{\gamma_\Sigma^{\mathrm{SC}}}(z) = \mathcal{M}^2_{\gamma_\alpha^{\mathrm{SC}}}(z)$. Like (14), the PIEP of RIM-OFDM-SC is represented by

$$\begin{aligned} \overline{P}_I^{\mathrm{SC}} &\leqslant \tfrac{\vartheta}{12}\left[\mathcal{M}_{\gamma_\Sigma^{\mathrm{SC}}}\left(-\tfrac{1}{4}\right) + 3\mathcal{M}_{\gamma_\Sigma^{\mathrm{SC}}}\left(-\tfrac{1}{3}\right)\right], \\ &= \tfrac{\vartheta}{12} L^2 \left(\overline{P}_{I_1}^{\mathrm{SC}} + 3\overline{P}_{I_2}^{\mathrm{SC}}\right), \end{aligned} \tag{25}$$

where $\overline{P}_{I_1}^{\mathrm{SC}}$ and $\overline{P}_{I_2}^{\mathrm{SC}}$ are determined by

$$\begin{aligned} \overline{P}_{I_1}^{\mathrm{SC}} &= \left[\sum_{l=0}^{L-1} \binom{L-1}{l} \tfrac{4(-1)^l}{4l+4+\bar{\gamma}}\right]^2, \\ \overline{P}_{I_2}^{\mathrm{SC}} &= \left[\sum_{l=0}^{L-1} \binom{L-1}{l} \tfrac{3(-1)^l}{3l+3+\bar{\gamma}}\right]^2. \end{aligned} \tag{26}$$

3.2.2. M-ary modulated symbol error probability

The same as (16), the instantaneous SEP of the M-ary modulated symbol for the RIM-OFDM-SC system is given by

$$\overline{P}_M^{\mathrm{SC}} \approx \frac{L^K}{6}\left(\overline{P}_{M_1}^{\mathrm{SC}} + 3\overline{P}_{M_2}^{\mathrm{SC}}\right), \tag{27}$$

where $\overline{P}_{M_1}^{\mathrm{SC}}$ and $\overline{P}_{M_2}^{\mathrm{SC}}$ are defined respectively by

$$\begin{aligned} \overline{P}_{M_1}^{\mathrm{SC}} &= \left[\sum_{l=0}^{L-1} \binom{L-1}{l} \tfrac{(-1)^l}{l+1+\rho\bar{\gamma}}\right]^K, \\ \overline{P}_{M_2}^{\mathrm{SC}} &= \left[\sum_{l=0}^{L-1} \binom{L-1}{l} \tfrac{3(-1)^l}{3l+3+4\rho\bar{\gamma}}\right]^K. \end{aligned} \tag{28}$$

As a result, the close-form expression for the average SEP of RIM-OFDM-SC is obtained by

$$\bar{P}_s^{\mathrm{SC}} \approx \frac{\vartheta L^2}{24}\left(\overline{P}_{I_1}^{\mathrm{SC}} + 3\overline{P}_{I_2}^{\mathrm{SC}}\right) + \frac{L^K}{12}\left(\overline{P}_{M_1}^{\mathrm{SC}} + 3\overline{P}_{M_2}^{\mathrm{SC}}\right). \tag{29}$$

Where each element $\overline{P}_{I_1}^{\mathrm{SC}}$, $\overline{P}_{I_2}^{\mathrm{SC}}$, $\overline{P}_{M_1}^{\mathrm{SC}}$, $\overline{P}_{M_2}^{\mathrm{SC}}$ is determined in (26) and (28), respectively.

4. Performance analysis Of RIM-OFDM-MRC/SC under imperfect CSI

4.1. Performance analysis for RIM-OFDM-MRC

In order to estimate the channel state information (CSI), the channel estimation methods for OFDM or MIMO-OFDM are not suitable for IM-OFDM because the sub-carrier indices are activated corresponding to the data bits, so the use of pilot symbol sequence is not effective to estimate channel. In the proposed scheme, the pilot-assisted channel estimation with low-pass interpolation (PSA-CE-LPI) can be utilized for channel estimation [25]. However, in practice channel estimation errors can occur at the receiver. In this section, we derive the closed-form expressions and evaluate the SEP performance of RIM-OFM-MRC and RIM-OFDM-SC in the presence of channel estimation error at the receiver. The receiver utilizes the actually estimated channel matrix in place of the perfect $\mathbf{H}$ in (3) to decode the transmitted signals. The estimated channel matrix $\tilde{\mathbf{H}}$ is expressed as $\tilde{\mathbf{H}} = \mathbf{H} - \mathbf{E}$, where $\tilde{\mathbf{H}} = \left[\tilde{\mathbf{H}}_1^T, \ldots, \tilde{\mathbf{H}}_L^T\right]^T$, for $\tilde{\mathbf{H}}_l = \mathrm{diag}\left(\tilde{h}_l(1), \ldots, \tilde{h}_l(N)\right)$, is the channel matrix when the CSI is imperfect, and $\mathbf{E} = \left[\mathbf{E}_1^T, \ldots, \mathbf{E}_L^T\right]^T$, where $\mathbf{E}_l = (e_l(1), \ldots, e_l(N))$, denotes the channel estimation error matrix which has independence with $\mathbf{H}$. Their distributions follow the Gaussian law $e_l(\alpha) \sim \mathcal{CN}(0, \epsilon^2), \tilde{h}_l(\alpha) \sim \mathcal{CN}(0, 1-\epsilon^2)$, where $\alpha = 1, 2, \ldots, N, \epsilon^2 \in [0, 1]$ represents the error variance. Using $\tilde{\mathbf{H}}$ the received signal from L antennas is given by

$$\widehat{\mathbf{y}} = \tilde{\mathbf{H}}^H \mathbf{y} = \tilde{\mathbf{H}}^H \mathbf{H} \boldsymbol{\lambda} s + \tilde{\mathbf{H}}^H \mathbf{n} = \widehat{\mathbf{H}}\, \boldsymbol{\lambda} s + \widehat{\mathbf{n}}, \tag{30}$$

where $\widehat{\mathbf{H}} = \tilde{\mathbf{H}}^H \mathbf{H}$ and $\widehat{\mathbf{n}} = \tilde{\mathbf{H}}^H \mathbf{n}$.

Under imperfect CSI condition, the estimated signal at the receiver using the ML detector can be represented by

$$(\tilde{\boldsymbol{\lambda}}, \tilde{s}) = \arg\min_{\boldsymbol{\lambda}, s} \left\| \mathbf{y} - \tilde{\mathbf{H}} \boldsymbol{\lambda} s \right\|^2. \tag{31}$$

The received signal $\mathbf{y}$ can be rewritten as

$$\mathbf{y} = \tilde{\mathbf{H}} \boldsymbol{\lambda} s + \tilde{\mathbf{n}}, \tag{32}$$

where $\tilde{\mathbf{n}} = \left(\mathbf{H} - \tilde{\mathbf{H}}\right)\boldsymbol{\lambda} s + \mathbf{n}; \tilde{\mathbf{n}} = [\tilde{n}(1), \ldots, \tilde{n}(N)]^T$ and $\tilde{n}(\alpha) \sim \mathcal{CN}(0, N_0)$ for $\alpha \in \theta_i; \tilde{n}(\alpha) = e(\alpha)s + n(\alpha)$ with the distribution $\tilde{n}(\alpha) \sim \mathcal{CN}(0, (1+\bar{\gamma}\epsilon^2)N_0)$ for $\alpha \notin \theta_i$.

4.1.1. Index error probability

The PIEP under the channel $\tilde{\mathbf{H}}$ is now given by

$$\begin{aligned} P(\boldsymbol{\lambda}_i \to \boldsymbol{\lambda}_j) &= P\left(\|\mathbf{y} - \tilde{\mathbf{H}}\boldsymbol{\lambda}_i s\|^2 > \|\mathbf{y} - \tilde{\mathbf{H}}\boldsymbol{\lambda}_j s\|^2\right) \\ &= P\left(\|\tilde{\mathbf{n}}\|^2 > \left\|\tilde{\mathbf{H}}(\boldsymbol{\lambda}_\mathbf{i} - \boldsymbol{\lambda}_\mathbf{j})\mathbf{s} + \tilde{\mathbf{n}}\right\|^2\right) \\ &= \mathbf{P}\left(-2\Re\left\{\tilde{\mathbf{n}}^\mathbf{H}\tilde{\mathbf{H}}\boldsymbol{\lambda}_\mathbf{ij}\mathbf{s}\right\} > \left\|\tilde{\mathbf{H}}\boldsymbol{\lambda}_\mathbf{ij}\mathbf{s}\right\|^2\right), \end{aligned} \tag{33}$$

where $\boldsymbol{\lambda}_{ij} = \boldsymbol{\lambda}_i - \boldsymbol{\lambda}_j$. Assume that $\theta_{ij}^i = \{\alpha | \alpha \in \theta_i, \alpha \notin \theta_j\}, \theta_{ji}^j = \{\alpha | \alpha \in \theta_j, \alpha \notin \theta_i\}$ and $\theta_{ij} = \theta_{ij}^i \cup \theta_{ji}^j$ for $i \neq j = 1, 2, \ldots, c$. Following Eq. (33) and after manipulations, we have $-2\Re\left\{\tilde{\mathbf{n}}^H\tilde{\mathbf{H}}\boldsymbol{\lambda}_{ij}s\right\} \sim \mathcal{CN}\left(0, \left(\sum_{\alpha\in\theta_{ji}^j}\tilde{\gamma}_\alpha + (1+\bar{\gamma}\epsilon^2)\sum_{\alpha\in\theta_{ij}^i}\tilde{\gamma}_\alpha\right)N_0\right)$ and $\left\|\tilde{\mathbf{H}}\boldsymbol{\lambda}_{ij}s\right\|^2 = \left(N_0\sum_{\alpha\in\theta_{ij}}\tilde{\gamma}_\alpha\right)$, where $\tilde{\gamma}_\alpha = \bar{\gamma}\left|\tilde{h}(\alpha)\right|^2$ is the instantaneous SNR of sub-carrier α under the imperfect CSI. The PIEP in (33) now can be described by

$$P(\boldsymbol{\lambda}_i \to \boldsymbol{\lambda}_j) = Q\left(\sqrt{\frac{\sum_{\alpha\in\theta_{ij}}\tilde{\gamma}_\alpha}{2\left(1 + \frac{\sum_{\alpha\in\theta_{ji}^j}\tilde{\gamma}_\alpha}{\sum_{\alpha\in\theta_{ij}}\tilde{\gamma}_\alpha}\bar{\gamma}\epsilon^2\right)}}\right) \approx Q\left(\sqrt{\frac{\sum_{\alpha\in\theta_{ij}}\tilde{\gamma}_\alpha}{2+\bar{\gamma}\epsilon^2}}\right). \tag{34}$$

For simplicity, $\sum_{\alpha\in\theta_{ji}^j}\tilde{\gamma}_\alpha / \sum_{\alpha\in\theta_{ij}}\tilde{\gamma}_\alpha$ in (34) is approximated to 1/2. The instantaneous PIEP always depends on the conditional PIEP $P(\boldsymbol{\lambda}_i \to \boldsymbol{\lambda}_j)$, so that $|\theta_{ij}|$ is minimized, i.e., $|\theta_{ij}| = 2$ since $|\theta_{ij}| = 2D \geqslant 2$. Denote $\Omega_i = \{j\}$ such that $|\theta_{ij}| = 2$ and its elements $\eta_i = |\Omega_i|$. Following (9), the PIEP of RIM-OFDM-MRC in the case of imperfect CSI can be expressed as

$$\tilde{P}_I^{\text{MRC}} \leqslant \frac{1}{c}\sum_{i=1}^{c}\sum_{j\in\Omega_i}\mathbb{E}_{\tilde{\gamma}_\Sigma^{\text{MRC}}}\left\{Q\left[\sqrt{\frac{\tilde{\gamma}_\Sigma^{\text{MRC}}}{2+\bar{\gamma}\epsilon^2}}\right]\right\}, \tag{35}$$

where $\tilde{\gamma}_\Sigma^{\text{MRC}} = \tilde{\gamma}_\alpha^{\text{MRC}} + \tilde{\gamma}_{\tilde{\alpha}}^{\text{MRC}}, \alpha \in \theta_{ij}^i, \tilde{\alpha} \in \theta_{ji}^j$. Then, applying the approximation of Q-function [27], the PIEP of RIM-OFDM-MRC under imperfect CSI can be rewritten as

$$\tilde{P}_I^{\text{MRC}} \approx \mathbb{E}_{\tilde{\gamma}_\Sigma^{\text{MRC}}}\left\{\vartheta\left(\frac{1}{12}e^{-\frac{\tilde{\gamma}_\Sigma^{\text{MRC}}}{2\left(2+\bar{\gamma}\epsilon^2\right)}} + \frac{1}{4}e^{-\frac{\tilde{\gamma}_\Sigma^{\text{MRC}}}{3\left(2+\bar{\gamma}\epsilon^2\right)}}\right)\right\}. \tag{36}$$

Based on the MGF definition in [26], the MGF of $\tilde{\gamma}$ can be expressed as $\mathcal{M}_{\tilde{\gamma}}(z) = \left[1 - \bar{\gamma}(1-\epsilon^2)z\right]^{-1}$.

The MGF of $\tilde{\gamma}_\Sigma^{\text{MRC}}$ can be given by

$$\mathcal{M}_{\tilde{\gamma}_\Sigma^{\text{MRC}}}(z) = \mathcal{M}_{\tilde{\gamma}}^{2L}(z) = \left[1 - \bar{\gamma}(1-\epsilon^2)z\right]^{-2L}. \tag{37}$$

Then, the closed-form expression for the average PIEP of RIM-OFDM-MRC in the imperfect CSI case is represented as

$$\begin{aligned} \tilde{P}_I^{\text{MRC}} &\leqslant \frac{\vartheta}{12}\mathbb{E}_{\tilde{\gamma}_\Sigma^{\text{MRC}}}\left\{e^{-\frac{\tilde{\gamma}_\Sigma^{\text{MRC}}}{2\left(2+\bar{\gamma}\epsilon^2\right)}} + 3e^{-\frac{2\tilde{\gamma}_\Sigma^{\text{MRC}}}{3\left(2+\bar{\gamma}\epsilon^2\right)}}\right\} \\ &= \frac{\vartheta}{12}\left[\mathcal{M}_{\tilde{\gamma}_\Sigma^{\text{MRC}}}\left(\frac{-1}{4+2\bar{\gamma}\epsilon^2}\right) + 3\mathcal{M}_{\tilde{\gamma}_\Sigma^{\text{MRC}}}\left(\frac{-2}{6+3\bar{\gamma}\epsilon^2}\right)\right] \\ &= \frac{\vartheta}{12}\left[\left(\frac{4+2\bar{\gamma}\epsilon^2}{4+\bar{\gamma}+\bar{\gamma}\epsilon^2}\right)^{2L} + 3\left(\frac{6+3\bar{\gamma}\epsilon^2}{6+2\bar{\gamma}+\bar{\gamma}\epsilon^2}\right)^{2L}\right]. \end{aligned} \tag{38}$$

4.1.2. M-ary modulated symbol error probability

Similar to the case of perfect CSI, the average error probability of the M-ary modulated symbol under the imperfect CSI is given by

$$\tilde{P}_M^{\text{MRC}} \approx 2Q\left(\sqrt{2\tilde{\gamma}_{\Sigma\alpha}^{\text{MRC}}}\sin(\pi/M)\right), \tag{39}$$

where $\tilde{\gamma}_{\Sigma\alpha}^{\text{MRC}} = \sum_{l=1}^{L}\sum_{k=1}^{K}\tilde{\gamma}_{l,\alpha_k}$. Since the distribution of the noise caused by imperfect CSI is represented as $\tilde{n}(\alpha) \sim \mathcal{CN}(0, N_0(1+\bar{\gamma}\varepsilon^2))$, and K active sub-carriers transmit the same data symbol s, the symbol s will be estimate with an instantaneous SNR given by $\tilde{\gamma}_{\Sigma\alpha}^{\text{MRC}} = \sum_{\alpha\in\theta}\tilde{\gamma}_\alpha^{\text{MRC}}/(N_0(1+\bar{\gamma}\varepsilon^2))$.

Based on the approximation of Q-fuction, we have

$$\tilde{P}_M^{\text{MRC}} \approx \frac{1}{6}\left(e^{-\rho\tilde{\gamma}_{\Sigma\alpha}^{\text{MRC}}} + 3e^{-\frac{4\rho\tilde{\gamma}_{\Sigma\alpha}^{\text{MRC}}}{3}}\right). \tag{40}$$

Applying the MGF of $\tilde{\gamma}$, we attain the MGF of $\tilde{\gamma}_{\Sigma\alpha}^{\text{MRC}}$ as follows

$$\mathcal{M}_{\tilde{\gamma}_{\Sigma\alpha}^{\text{MRC}}}(s) = \mathcal{M}_{\tilde{\gamma}}^{LK}(s) = \left(1 - \bar{\gamma}(1-\epsilon^2)s\right)^{-LK}. \tag{41}$$

The M-ary modulated symbol error probability of the RIM-OFDM-MRC is given by

$$\tilde{P}_M^{\text{MRC}} \approx \frac{1}{6}\left[\frac{1}{\left(1 + \frac{(1-\epsilon^2)\bar{\gamma}\rho}{1+\bar{\gamma}\epsilon^2}\right)^{LK}} + \frac{3}{\left(1 + \frac{4(1-\epsilon^2)\bar{\gamma}\rho}{3(1+\bar{\gamma}\epsilon^2)}\right)^{LK}}\right]. \tag{42}$$

Accordingly, the average SEP for RIM-OFDM-MRC under the imperfect CSI can be expressed as

$$\begin{aligned} \tilde{P}_s^{\text{MRC}} &= \frac{\vartheta}{24}\left[\left(\frac{4+2\bar{\gamma}\varepsilon^2}{4+\bar{\gamma}+\bar{\gamma}\varepsilon^2}\right)^{2L} + 3\left(\frac{6+3\bar{\gamma}\varepsilon^2}{6+2\bar{\gamma}+\bar{\gamma}\varepsilon^2}\right)^{2L}\right] \\ &\quad + \frac{1}{12}\left[\frac{1}{\left(1 + \frac{(1-\varepsilon^2)\bar{\gamma}\rho}{1+\bar{\gamma}\varepsilon^2}\right)^{LK}} + \frac{3}{\left(1 + \frac{4(1-\varepsilon^2)\bar{\gamma}\rho}{3(1+\bar{\gamma}\varepsilon^2)}\right)^{LK}}\right]. \end{aligned} \tag{43}$$

It can be realized that when $\epsilon^2 = 0$, $\tilde{P}_s^{\text{MRC}}$ in (43) is equal to $\overline{P_s}^{\text{MRC}}$ in (21). Especially, when $\epsilon^2 > 0$, the SEP of RIM-OFDM-MRC is higher than that in the perfect CSI condition, the reliability of the system considerably decreased in comparison with the case of certain CSI.

4.1.3. Asymptotic analysis

The asymptotic analysis for the SEP of RIM-OFDM-MRC under uncertain CSI provides an important insight into the behavior of the system when being affected by different CSIs. In large SNR, for $\epsilon^2 > 0$, we have

$$\begin{aligned} \tilde{P}_s^{\text{MRC}} &\approx \frac{\vartheta}{24}\left[\left(\frac{2\epsilon^2}{1+\epsilon^2}\right)^{2L} + \left(\frac{3\epsilon^2}{2+\epsilon^2}\right)^{2L}\right] \\ &\quad + \frac{1}{12}\left[\left(\frac{1+\epsilon^2}{\epsilon^2+\omega\rho}\right)^{LK} + 3\left(\frac{3\epsilon^2}{3\epsilon^2+4\omega\rho}\right)^{LK}\right], \end{aligned} \tag{44}$$

where $\omega = 1 - \epsilon^2$. It can be seen from (44) that, for large SNRs, $\tilde{P}_s^{\text{MRC}}$ only depends on ϵ^2, N, K and M, without be affected by $\bar{\gamma}$. Also, the SEP increases when increasing ϵ^2. An irreducible error floor occurs at high ϵ^2 and the system does not achieve diversity gain. The same statement can be drawn for the RIM-OFDM-SC scheme.

4.2. Performance analysis for RIM-OFDM-SC

4.2.1. Index error probability

Similar to above analysis for RIM-OFDM-SC under perfect CSI, the MGF of $\tilde{\gamma}_\alpha^{\text{SC}}$ is given by

$$\mathcal{M}_{\tilde{\gamma}_\alpha^{SC}}(z) = L\sum_{l=0}^{L}\binom{L-1}{l}\frac{(-1)^l}{l+1-z(1-\epsilon^2)\bar{\gamma}}. \quad (45)$$

Following (26), the approximated PIEP of RIM-OFDM-SC under the imperfect CSI is expressed by

$$\tilde{P}_I^{SC} \leqslant \frac{\vartheta}{12}\left[\mathcal{M}_{\tilde{\gamma}_\Sigma^{SC}}\left(\frac{-1}{4+2\bar{\gamma}\epsilon^2}\right)+3\mathcal{M}_{\tilde{\gamma}_\Sigma^{SC}}\left(\frac{-2}{6+3\bar{\gamma}\epsilon^2}\right)\right] = \frac{\vartheta}{12}L^2\left(\tilde{P}_{I_1}^{SC}+3\tilde{P}_{I_2}^{SC}\right), \quad (46)$$

where $\tilde{P}_{I_1}^{SC}, \tilde{P}_{I_2}^{SC}$ are determined by

$$\tilde{P}_{I_1}^{SC} = \left[\sum_{l=0}^{L-1}\binom{L-1}{l}\frac{(4+2\bar{\gamma}\epsilon^2)(-1)^l}{(4+2\bar{\gamma}\epsilon^2)l+4+\bar{\gamma}+\bar{\gamma}\epsilon^2}\right]^2,$$
$$\tilde{P}_{I_2}^{SC} = \left[\sum_{l=0}^{L-1}\binom{L-1}{l}\frac{(6+3\bar{\gamma}\epsilon^2)(-1)^l}{(6+3\bar{\gamma}\epsilon^2)l+6+2\bar{\gamma}+\bar{\gamma}\epsilon^2}\right]^2. \quad (47)$$

4.2.2. M-ary modulated symbol error probability

Similar to (27), the M-ary modulated SEP for RIM-OFDM-SC in the case of imperfect CSI can be represented by

$$\tilde{P}_M^{SC} \approx \frac{L^K}{6}\left(\tilde{P}_{M_1}^{SC}+3\tilde{P}_{M_2}^{SC}\right), \quad (48)$$

where $\tilde{P}_{M_1}^{SC}$ and $\tilde{P}_{M_2}^{SC}$ are respectively given by

$$\tilde{P}_{M_1}^{SC} = \left[\sum_{l=0}^{L-1}\binom{L-1}{l}\frac{(-1)^l}{l+1+\frac{\rho(1-\epsilon^2)\bar{\gamma}}{1+\bar{\gamma}\epsilon^2}}\right]^K,$$
$$\tilde{P}_{M_2}^{SC} = \left[\sum_{l=0}^{L-1}\binom{L-1}{l}\frac{3(-1)^l}{3l+3+\frac{4\rho(1-\epsilon^2)\bar{\gamma}}{1+\bar{\gamma}\epsilon^2}}\right]^K. \quad (49)$$

Accordingly, from (19), (46) and (48), the average SEP of RIM-OFDM-SC under imperfect CSI case is represented by

$$\tilde{P}_s^{SC} \approx \frac{L^2\sum_{i=1}^{c}\eta_i}{24c}\left(\tilde{P}_{I_1}^{SC}+3\tilde{P}_{I_2}^{SC}\right)+\frac{L^K}{12}\left(\tilde{P}_{M_1}^{SC}+3\tilde{P}_{M_2}^{SC}\right), \quad (50)$$

where $\tilde{P}_{I_1}^{SC}$, $\tilde{P}_{I_2}^{SC}$, and $\tilde{P}_{M_1}^{SC}, \tilde{P}_{M_2}^{SC}$ are given in (47) and (49), respectively.

4.3. Extention to MIMO configuration

The proposed scheme is considered under point-to-point communication scenario where the complexity is significantly required. However, this proposal can be applied to the MIMO system where the transmitter and receiver are equipped multiple antennas. The MIMO configuration can be implemented as in [18]. The transmitter uses T transmit antennas and the receiver is equipped with L receive antennas. The incoming data bits is divided into T groups and applying the IM-OFDM principle to each branch of MIMO transmitter, consisting of index mapping and M-ary modulation. However, the same modulated data symbol is transmitted over the active sub-carriers. At each branch of the transmitter, IM-OFDM sub-block is construct and then G sub-blocks are combined to generate IM-OFDM block.

At the receiver, the maximum likelihood (ML) detector is used to jointly estimate the active sub-carriers and corresponding data symbol in each sub-block. The ML detector can simultaneously search over T transmit antennas. However, the limitation of ML detector is the high complexity, thus we can employ the minimum mean square error (MMSE), MMSE with log-likelihood ratio (MMSE-LLR). In order to effectively deal with interference, ordered successive interference cancellation (OSIC) based MMSE-LLR (OSIC-MMSE-LLR) can be utilized as in [18].

5. Performance evaluation and discussion

This section reports the analytical and Monte-Carlo simulation results to prove the performance of RIM-OFDM-MRC/SC systems in the different cases of CSI. We choose the existing IM-OFDM-MRC/SC as the reference system. It is assumed that the channel over each sub-carrier suffers from flat Rayleigh fading. In addition, the ML detection is utilized for all considered systems. The IM-OFDM system with a total of N sub-carriers, K active sub-carriers and modulation order M is referred to as (N, K, M).

5.1. Performance evaluation under perfect CSI

Fig. 2 illustrates the comparison between SEP performance of RIM-OFDM-MRC and the IM-OFDM-MRC [16] at the spectral efficiency of 1 bps/Hz and 1.25 bps/Hz. As realized from Fig. 2, at the same and even the larger spectral efficiency, the transmission reliability of proposed scheme outperforms the reference system. Comparing the two results, it can be seen that at the spectral efficiency of 1.25 bps/Hz and the SEP of 10^{-4}, the RIM-OFDM-MRC achieves SNR gains of more than 6 dB over IM-OFDM-MRC. A possible explanation for this might be that the RIM-OFDM-MRC uses $L = 2$ receive antennas, it can achieve the maximum diversity order of $2L = 4$. The performance improvement is attained by jointly attaining the frequency and spatial diversity. The proposed scheme achieves double diversity gain compared with that of IM-OFDM-MRC which exploits the spatial diversity only. Analytical bounds are tightly close with the simulation curves in high SNRs for different configurations. The exact expressions in (21) and (22) are thus verified. The asymptotic analysis result in (22) has proved that the maximum diversity order of RIM-OFDM-MRC is limited to $2L$ and the same observation is attained for RIM-OFDM-SC as in the following Fig. 3.

Fig. 3 compares between the SEP performance of the RIM-OFDM-SC and the IM-OFDM-SC system with $N = 4$, $K = 2$, $L = 2$ and $M = \{4, 8\}$. It can be observed that at higher spectral efficiency, the RIM-OFDM-SC system also achieves substantially enhanced

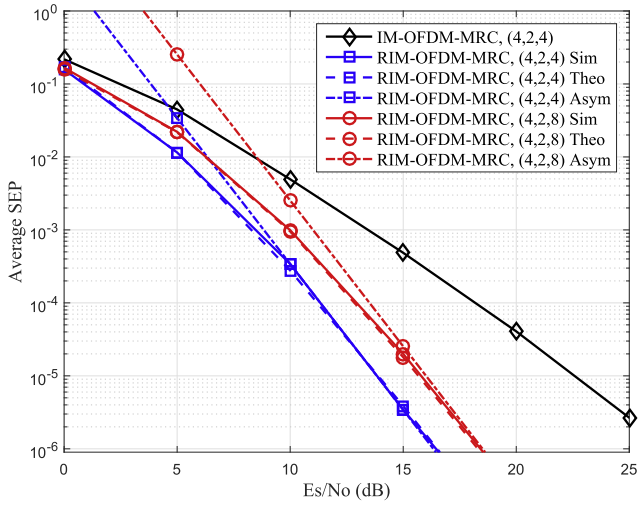

Fig. 2. SEP comparison between RIM-OFDM-MRC and the conventional IM-OFDM-MRC for $N = 4$, $K = 2$, $L = 2$, $M = \{4, 8\}$.

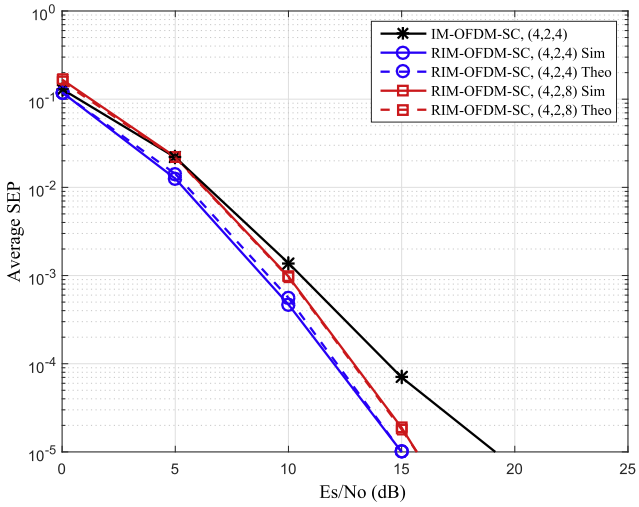

Fig. 3. SEP performance of RIM-OFDM-SC in comparison with IM-OFDM-SC for $N = 4,\ K = 2,\ L = 2,\ M = \{4, 8\}$.

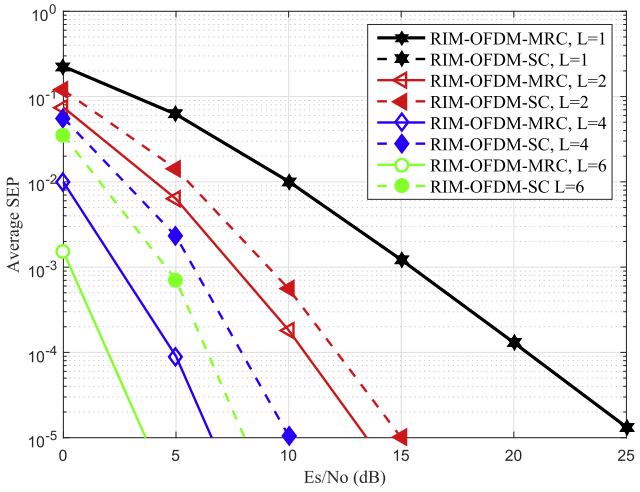

Fig. 5. Impact of L on the SEP performance of RIM-OFDM-MRC and RIM-OFDM-SC for $M = 4,\ N = 4,\ K = 2$ and $L = \{1, 2, 4, 6\}$.

SEP performance in comparison with the IM-OFDM-SC. In particular, an improvement of 2 dB can be achieved at the SEP of 10^{-4}.

As realized from Fig. 3, with different $M,\ N,\ L$ and K, the curves obtained by the approximated SEPs given in (29) matches well with simulation ones. This certainly verifies our theoretical analysis.

The relationship between the index error probability (IEP) of RIM-OFDM-MRC/SC and the modulation order M in comparison with IM-OFDM-MRC/SC is presented in Fig. 4. As shown in this figure, no differences were found among the IEPs when increasing M. This result may be explained by the fact that the IEP does not depend on the modulation order M, but only on the energy per symbol, i.e., φE_s. The IEP performance of the two proposed schemes outperforms that of IM-OFDM-MRC/SC by about 2 dB. Beside that, the very tight IEP curves in the figure verifies our analysis in (14) and (25).

Impacts of the number of spatial diversity branches on the SEP of the proposed systems can be found in Fig. 5. It can be seen that the SEP performance of both RIM-OFDM-MRC and RIM-OFDM-SC are significantly improved when increasing the number of spatial diversity branches. In addition, the SEP performance curves of the two schemes have the same gradient, which implicates that they have the equal diversity order. Remark 1 is validated. Nevertheless, the RIM-OFDM-MRC system attains better performance than RIM-OFDM-SC. Particularly, at SEP of 10^{-4}, RIM-OFDM-MRC gains 3 dB over RIM-OFDM-SC. Whereas, the scheme using SC can achieve lower complexity than the MRC. Thus, depending on each specific system, either MRC or SC is selected flexibly.

Figs. 6 and 7 illustrate the influence of the number of active subcarriers on the SEP of RIM-OFDM-MRC and RIM-OFDM-SC. We can see that at the same spectral efficiency, the average SEP of the RIM-OFDM-MRC system increases with increasing K. The best SEP performance can be achieved when $K = 2$. The same observation also can be made for RIM-OFDM-SC. Hence, this recommends to choose K not larger than 2 for the best RIM-OFDM-MRC/SC configuration. However, this statement is no longer true when the spectral efficiency is not the same as illustrated in Figs. 6 and 7. While small K is the best selection when system uses low modulation order, i.e., small M. At a large M, the best SEP performance is attained with a large K. In conclusion, the best configuration should be designed with K not larger than 2 for small M, $(M \leqslant 8)$ and large K for large M, $(M \geqslant 16)$. This validates Remark 3.

The influence of modulation size on the SEP of RIM-OFDM-MRC/SC when $N = 5,\ K = 4$, and $M = \{2, 4, 8, 16, 32\}$ can be found in Fig. 8. As shown in this figure, at high SNRs, very little difference

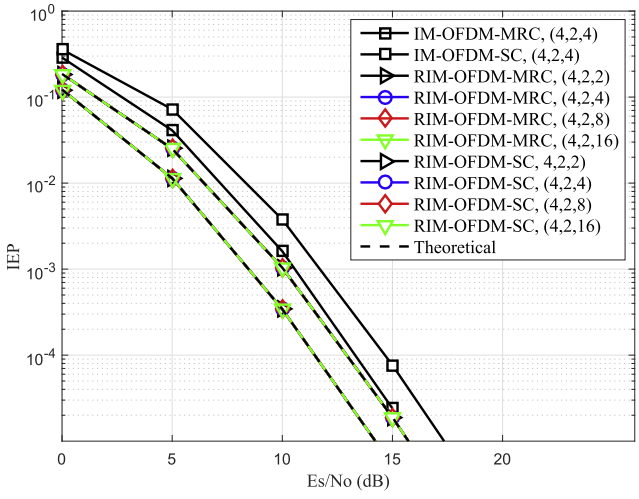

Fig. 4. The relationship between the index error probability of RIM-OFDM-MRC/SC and the modulation order M in comparison with IM-OFDM-MRC/SC for $N = 4, K = 2, M = \{2, 4, 8, 16\}$.

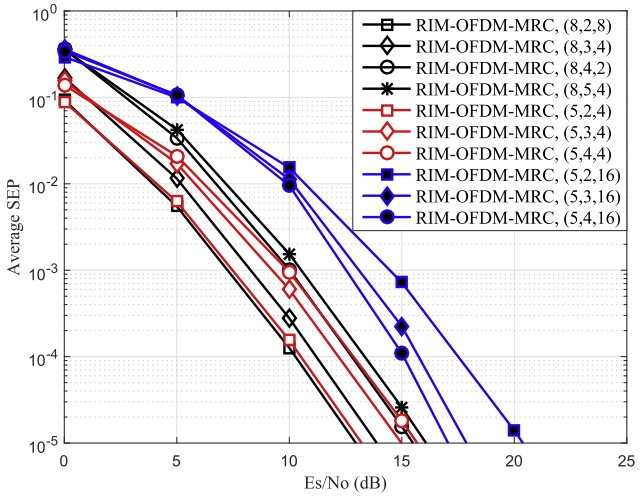

Fig. 6. The SEP performance of RIM-OFDM-MRC under influence of K for $M = \{2, 4, 8, 16\},\ N = \{5, 8\},\ K = \{2, 3, 4, 5\}$.

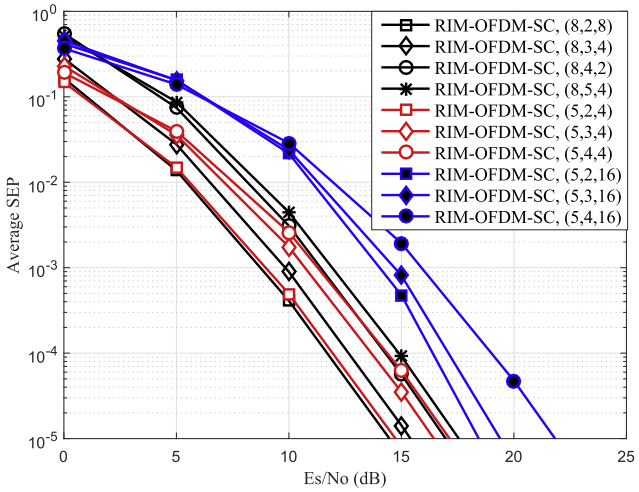

Fig. 7. The SEP performance of RIM-OFDM-SC under influence of K when $M = \{2, 4, 8, 16\}, N = \{5, 8\},\ K = \{2, 3, 4, 5\}$.

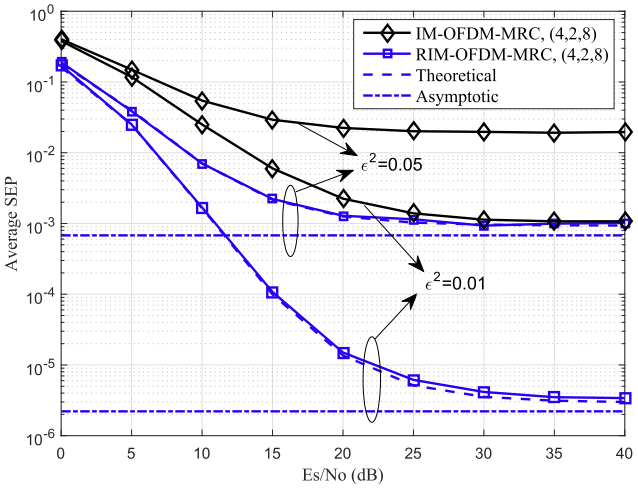

Fig. 9. SEP performance of RIM-OFDM-MRC in comparison with IM-OFDM-MRC under imperfect CSI when $N = 4,\ K = 2,\ M = \{4, 8\}$, and $\epsilon^2 = \{0.01, 0.05\}$.

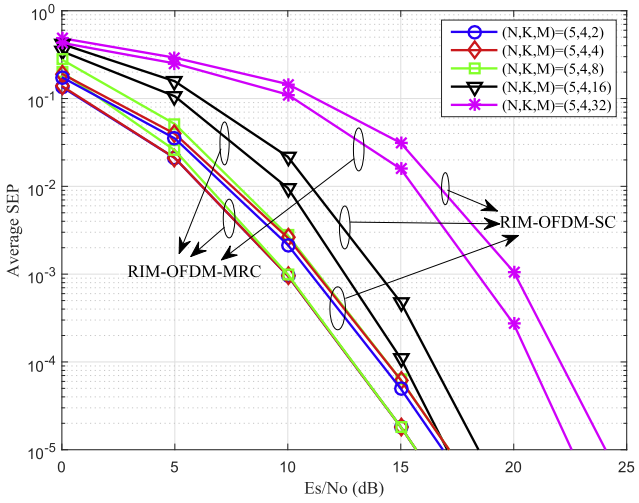

Fig. 8. Influence of modulation size on the SEP of RIM-OFDM-MRC/SC for $N = 5,\ K = 4$, and $M = \{2, 4, 8, 16, 32\}$.

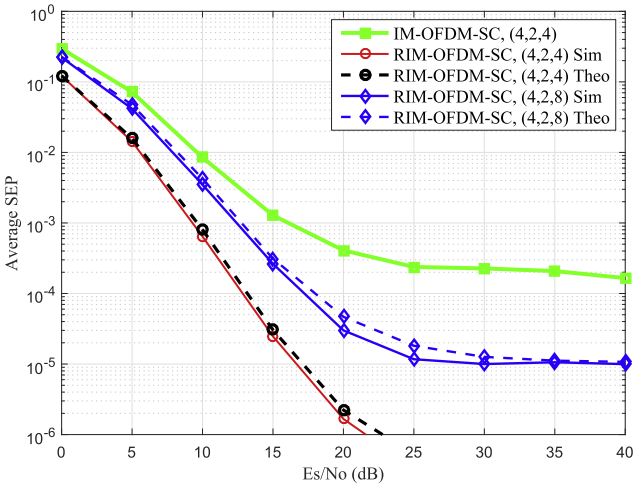

Fig. 10. SEP performance of RIM-OFDM-SC in comparison with IM-OFDM-SC under imperfect CSI when $N = 4,\ K = 2,\ M = \{4, 8\}$, and $\epsilon^2 = 0.01$.

can be found in the SEPs of both RIM-OFDM-MRC/SC when the value of M is small ($M \leq 8$). The significant difference was only evident when $M \geqslant 16$. This means that the SEP is unaffected by modulation order when M is small, it is only affected by the index estimation.

5.2. SEP performance evaluation under imperfect CSI condition

Fig. 9 and 10 depict the SEP performance of RIM-OFDM-MRC and RIM-OFDM-SC when channel estimation errors occur at the receiver with error variance $\epsilon^2 = \{0.01, 0.05\}$. Importantly, even under imperfect CSI condition, RIM-OFDM-MRC/SC still achieves better SEP performance than the conventional IM-OFDM-MRC/SC at the same spectral efficiency. Since the value of ϵ^2 is fixed, the error floor occurs in both the RIM-OFDM-MRC and RIM-OFDM-SC schemes. The analytical results in Eqs. (43) and (50) close tightly with the simulation results. This validates the theoretical derivation.

5.3. Comparison of the computational complexity

The calculation complexity of proposed scheme is investigated by the number of floating point operations (flops) per sub-block. Assume that a flop can stands for a real subtraction, a real multiplication, or a real summation. A complex summation and a complex multiplication are presented by 2 flops and 6 flops, respectively. Based on these assumptions, the complexity is calculated as follows

$$\mathcal{C}_{\text{RIM-OFDM-MRC}} = 2N + 6LN + (4N + 2NL + 5)cM^K + cM^K - 1. \quad (51)$$

$$\mathcal{C}_{\text{IM-OFDM-MRC}} = 6LN + (2N + 2NL + 5)cM^K + cM^K - 1. \quad (52)$$

$$\mathcal{C}_{\text{RIM-OFDM-SC}} = 8N + N(5L - 1) + (6N + 5)cM^K + cM^K - 1. \quad (53)$$

$$\mathcal{C}_{\text{IM-OFDM-SC}} = 6N + N(5L - 1) + (4N + 5)cM^K + cM^K - 1 \quad (54)$$

It can be seen that the proposed scheme has higher computational complexity than the IM-OFDM with diversity reception. It lies on $2N$ flops of the repetition of transmitted data symbols at the transmitter. It is also the limitation of our proposal. The proposed scheme can achieve a much better error performance at not much higher complexity than the IM-OFDM-MRC/SC. Beside that, RIM-OFDM-MRC has the larger complexity than RIM-OFDM-SC.

6. Conclusions

This paper has clarified the advantage of two enhanced IM-OFDM schemes, namely RIM-OFDM-MRC and RIM-OFDM-SC,

which can outperform the conventional IM-OFDM-MRC and IM-OFDM-SC system at the same spectral efficiency thanks to simultaneously achievable spatial and frequency diversities. Using mathematical approximations, we have also successfully determined the closed-form expressions of the index and symbol error probability for both RIM-OFDM-MRC and RIM-OFDM-SC under different conditions of channel state information.

The theoretical results have important implications as a convenient framework for examining the system reliability under various configurations and channel conditions. The analytical and simulation results also prove that our proposed schemes can yield substantially better performance than the benchmark systems at the same spectral efficiency even when CSI is known incorrectly at the receiver. With their simplicity and effectiveness, the proposed schemes can be suitable for the wireless applications that require low complexity and high transmission reliability.

Acknowledgement

This work is sponsored by National Foundation for Science and Technology Development (Nafosted) under project number 102.02-2015.23.

Appendix A. Supplementary material

Supplementary data associated with this article can be found, in the online version, at https://doi.org/10.1016/j.aeue.2019.05.022.

References

[1] Torabi M. Adaptive modulation for spacefrequency block coded OFDM systems. AEU-Int J Electron Commun 2008;62(7):521–33.
[2] Djeddou M, Berrahma F, Ghanem K. Improved Spectral Efficiency of SM-OFDM Using a Set of Rotated Constellations. AEU-Int J Electron Commun 2018;93:317–24.
[3] Singh D, Joshi HD. Error probability analysis of STBC-OFDM systems with CFO and imperfect CSI over generalized fading channels. AEU-Int J Electron Commun 2019;98:156–63.
[4] Basar E, Aygl, Panayrc E, Poor HV. Orthogonal frequency division multiplexing with index modulation. IEEE Trans Commun Signal Process 2013;61(22):5536–49.
[5] Abu-Alhiga R, Haas H. Subcarrier-index modulation OFDM. Proceedings of IEEE 20th international symposium on personal, indoor and mobile radio communications (PIMRC), vol. 18. p. 177–81.
[6] Xiao Y, Wang S, Dan L, Lei X, Yang P, Xiang W. OFDM with interleaved subcarrier-index modulation. IEEE Commun Lett 2014;18(8):1447–50.
[7] Fan R, Yu YJ, Guan YL. Improved orthogonal frequency division multiplexing with generalised index modulation. IET Commun 2016;10(8):969–74.
[8] Mao T, Wang Q, Wang Z. Generalized dual-mode index modulation aided OFDM. IEEE Commun Lett 2017;21(4):761–4.
[9] Wen M, Basar E, Li Q, Zheng B, Zhang M. Multiple-mode orthogonal frequency division multiplexing with index modulation. IEEE Trans Commun 2017;65(9):3892–906.
[10] Van Luong T, Ko Y. A tight bound on BER of MCIK-OFDM with greedy detection and imperfect CSI. IEEE Commun Lett 2017;21(12):2594–7.
[11] Van Luong T, Ko Y. Impact of CSI uncertainty on MCIK-OFDM: tight closed-form symbol error probability analysis. IEEE Trans Veh Technol 2018;67(2):1272–9.
[12] Ko Y. A tight upper bound on bit error rate of joint OFDM and multi-carrier index keying. IEEE Commun Lett 2014;18(10):1763–6.
[13] Van Luong T, Ko Y. Symbol error outage performance analysis of MCIK-OFDM over complex TWDP fading. In: Proceedings of 23th European wireless conference. p. 1–5. VDE.
[14] Basar E. OFDM with index modulation using coordinate interleaving. IEEE Wireless Commun Lett 2015;4(4):381–4.
[15] Wen M, Ye B, Basar E, Li Q, Ji F. Enhanced orthogonal frequency division multiplexing with index modulation. IEEE Trans Wireless Commun 2017;16(7):4786–801.
[16] Crawford J, Chatziantoniou E, Ko Y. On the SEP analysis of OFDM index modulation with hybrid low complexity greedy detection and diversity reception. IEEE Trans Veh Technol 2017;66(9):8103–18.
[17] Choi J. Coded OFDM-IM with transmit diversity. IEEE Trans Commun 2017;65(7):3164–71.
[18] Basar E. Multiple-input multiple-output OFDM with index modulation. IEEE Sig Process Lett 2015;22(12):2259–63.
[19] Wang L, Chen Z, Gong Z, Wu M. Space-frequency coded index modulation with linear-complexity maximum likelihood receiver in the MIMO-OFDM system. IEEE Sig Process Lett 2016;23(10):1439–43.
[20] Zheng B, Wen M, Basar E, Chen F. Multiple-input multiple-output OFDM with index modulation: low-complexity detector design. IEEE Trans Sig Process 2017;65(11):2758–72.
[21] Thanh HLT, Tran XN. Repeated index modulation for OFDM with space and frequency diversity. In: Proceedings of IEEE international conference on advanced technologies for communications (ATC). p. 97–102.
[22] Yu-Kuan C, Fang-Biau U, Ye-Shun S, Cheng-Hui Li. Joint channel estimation and turbo equalization for MIMO-OFDM-IM systems. Int Jour Electron 2018. https://doi.org/10.1080/00207217.2018.1553246.
[23] Andrews JG, Ghosh A, Muhamed R. Fundamentals of WiMAX: understanding broadband wireless networking. Edinburg, England: Pearson Education; 2007.
[24] Dahlman E, Parkvall S, Skold J. 4G: LTE/LTE-advanced for mobile broadband. USA: Academic Press; 2013.
[25] Acar Y, Colar SA, Basar E. Channel estimation for OFDM-IM systems; 2018. <http://online.journals.tubitak.gov.tr/openAcceptedDocument.htm?fileID=1070715&no=245672>.
[26] Simon MK, Alouini MS. Digital communication over fading channels. John Wiley & Sons; 2005.
[27] Chiani M, Dardari D, Simon MK. New exponential bounds and approximations for the computation of error probability in fading channels. IEEE Trans Wireless Commun 2003;2(4):840–5.